Drug Metabolism and Pharmacokinetics 30 (2015) 441–448

Contents lists available at ScienceDirect

Drug Metabolism and Pharmacokinetics

journal homepage: http://www.journals.elsevier.com/drug-metabolism-and-pharmacokinetics

Regular article

Pharmacokinetics and pharmacodynamics of mycophenolic acid in Nagase analbuminemic rats: Evaluation of protein binding effects using the modeling and simulation approach

Kazuaki Yoshimura [a, b], Ikuko Yano [a, b, *], Misaki Kawanishi [a, b], Shunsaku Nakagawa [b], Atsushi Yonezawa [b], Kazuo Matsubara [b]

[a] Department of Clinical Pharmacy and Education, Graduate School of Pharmaceutical Sciences, Kyoto University, Sakyo-ku, Kyoto 606-8501, Japan
[b] Department of Clinical Pharmacology and Therapeutics, Kyoto University Hospital, Sakyo-ku, Kyoto 606-8507, Japan

ARTICLE INFO

Article history:
Received 14 September 2015
Received in revised form
9 October 2015
Accepted 25 October 2015
Available online 3 November 2015

Keywords:
Mycophenolic acid
Inosine-5′-monophosphate dehydrogenase
Nagase analbuminemic rat
Nonlinear mixed effects modeling
UDP-Glucuronosyltransferase

ABSTRACT

This study aimed to examine the pharmacokinetics and pharmacodynamics of mycophenolic acid (MPA) in Nagase analbuminemic rats (NARs) to evaluate the effect of protein binding on the associated inosine-5′-monophosphate dehydrogenase (IMPDH) activity. Free fractions of MPA in the control rats and NARs were 2.09 and 24.8%, respectively. Pharmacokinetic and pharmacodynamic parameters simultaneously obtained by the nonlinear mixed effects modeling program NONMEM explained reasonably well the concentrations of MPA and MPA glucuronide as well as IMPDH activity in both rats. NARs showed a higher clearance and a smaller volume of distribution based on the free MPA concentration than the controls did, besides the increase in free fraction. The half-maximal inhibitory concentration based on free MPA was estimated as 163 ng/mL for both rats. Simulations based on the obtained pharmacokinetic and pharmacodynamic parameters showed that the area under the IMPDH activity-time curve decreased non-linearly according to the increase in free fraction of MPA. In conclusion, the experimental data obtained from NARs followed by the modeling and simulation approach quantitatively clarified that the free MPA concentration was suitable for the biomarker of immunosuppressive effect of MPA. Dose adjustments based on the total MPA may cause unnecessary overexposure to MPA in patients with hypoalbuminemia.

1. Introduction

Mycophenolic acid (MPA) selectively inhibits inosine-5′-monophosphate dehydrogenase (IMPDH), which catalyzes the rate-limiting step in the *de novo* synthesis of guanine nucleotide and suppresses the proliferation of B and T lymphocytes [1]. MPA is clinically used to suppress acute rejection after solid organ transplantation as well as graft-*versus*-host disease in hematopoietic stem cell transplantation [2,3], in the combination with other immunosuppressants such as a calcineurin inhibitor, tacrolimus or cyclosporine.

MPA is metabolized by uridine 5′-diphospho-glucuronosyltransferase (UGT) isoforms in the liver to an inactive MPA glucuronide (MPAG), which is mainly eliminated through the urine [3]. The pharmacokinetics of MPA is affected by changes in hepatic or renal functions [4] and shows a large inter- and intraindividual variability [5]. Therefore, patients who have had transplants followed by MPA administration should be managed by therapeutic drug monitoring of plasma MPA concentrations. The consensus target exposure range of MPA has been proposed as an area under the concentration-time curve (AUC) from 0 to 12 h of 30–60 μg h/mL based on the total plasma concentration in patients with renal transplants [6]. The target exposure range of MPA is possibly influenced by changes in plasma albumin concentrations, since the free fraction of MPA was 1–2% [7].

IMPDH activity in peripheral blood mononuclear cells (PBMCs) has been suggested as a surrogate biomarker for the

* Corresponding author. Department of Clinical Pharmacy and Education, Graduate School of Pharmaceutical Sciences, Kyoto University, Sakyo-ku, Kyoto, 606-8501, Japan.
E-mail addresses: yoshimura.kazuaki.52r@st.kyoto-u.ac.jp (K. Yoshimura), iyano@kuhp.kyoto-u.ac.jp (I. Yano), misaki.kawanishi@shionogi.co.jp (M. Kawanishi), nakashun@kuhp.kyoto-u.ac.jp (S. Nakagawa), ayone@kuhp.kyoto-u.ac.jp (A. Yonezawa), kmatsuba@kuhp.kyoto-u.ac.jp (K. Matsubara).

http://dx.doi.org/10.1016/j.dmpk.2015.10.004
1347-4367/

immunosuppressive effects of MPA, and pre-transplant IMPDH activity is associated with rejection in patients with renal transplants [8]. In a recent study, the area under the effect-time curve (AUEC) of IMPDH activity on day 21 after hematopoietic stem cell transplantation was found to be associated with cytomegalovirus reactivation, non-relapse mortality, and overall mortality [9]. Therefore, the measurement of IMPDH activity in addition to monitoring the AUC of total plasma MPA is considered an effective predictor of the clinical outcome of MPA therapy. However, little is known about the quantitative relationship between the free fraction of MPA in the plasma and IMPDH activity.

Nagase analbuminemic rats (NARs) are an established animal model for human familial analbuminemia [10]. NARs were used to examine the effect of decreased protein binding on the pharmacokinetics and pharmacodynamics of drugs having a high protein binding property, such as bumetanide [11], azosemide [12], and methotrexate [13]. NARs have also been utilized in the investigation of the toxicokinetics and toxicodynamics of clofibrate [14]. In this study, we constructed the simultaneous pharmacokinetic and pharmacodynamic model of MPA, and analyzed the experimental data obtained from NARs as well as control rats by the nonlinear mixed effects modeling method. The simulation study based on the obtained pharmacokinetic and pharmacodynamic parameters quantitatively evaluated the effect of protein binding on the IMPDH activity, as a biomarker of the pharmacodynamics of MPA.

2. Materials and methods

2.1. Chemicals

MPA and MPAG were purchased from Wako Pure Chemical Industries Ltd. (Osaka, Japan) and Analytical Services International Ltd. (London, UK), respectively. Xanthosine-5′-monophosphate (XMP) disodium salt was obtained from Santa Cruz Biotechnology Inc. (Santa Cruz, CA, USA). Adenosine-5′-monophosphate (AMP) sodium salt, inosine-5′-monophosphate disodium salt from yeast and nicotinamide adenine dinucleotide (NAD^+) were from Nacalai Tesque Inc. (Kyoto, Japan). All the chemicals used were of the highest grade available.

2.2. In vivo pharmacokinetic and pharmacodynamic study

Male Sprague-Dawley rats (control) and NARs (8- to 10-week-old and 9- to 11-week-old, respectively) were obtained from Japan SLC, Inc. (Osaka, Japan). Both groups of rats were anesthetized with intraperitoneal injections of 40 mg/kg pentobarbital sodium. A polyethylene tube was inserted into the femoral artery and vein. Then, MPA dissolved in 10% cremophor and 10% ethanol in saline was intravenously infused for 1 h via the femoral vein at doses of 0.5 or 5 and 5 or 15 mg/kg in the control and NAR groups, respectively. Blood samples (0.2 mL) were collected sequentially before and at 0.5, 1, 1.25, 1.5, 2, 2.5, 3, and 4 h after the start of MPA administration and were stored at 4 °C until completion of blood collection. The blood samples were centrifuged at 14,000 *g* for 5 min to obtain the plasma, and then plasma samples (100 μL) were acidified by adding 2 μL of 10% acetic acid for the assay of MPA and MPAG. The PBMCs, which were obtained from the residual blood samples by centrifuging at 1000 *g* for 15 min using Ficoll-Paque Premium 1.084 (GE Healthcare Bio-Sciences AB, Uppsala, Sweden), were frozen at −20 °C until measurements of IMPDH activity were performed. The free fraction of MPA and MPAG in both groups of rats was determined using plasma from blood samples collected 15 min after MPA administration. The plasma samples were ultrafiltrated (Amicon Ultra 30 K centrifugal filter devices, Merck Millipore Ltd., Carrigtwohill, Ireland) at 14,000 *g* for 10 min. The free MPA and MPAG concentrations were calculated by multiplying their respective total concentrations by the average of the free fraction of each drug for each group. All procedures were conducted in compliance with the Guidelines for Animal Experiments of the Kyoto University.

2.3. Analysis of cytochrome P450 enzyme (CYP) and UGT mRNA expressions using real-time polymerase chain reaction (PCR)

The total RNA was extracted from the liver using the RNeasy mini kit (Qiagen Inc., Valencia, CA, USA) according to the manufacturer's instruction and further quantitated using the BioSpec-nano spectrophotometer (Shimadzu, Kyoto, Japan) at a wavelength of 260 nm. The total RNA (1 μg) was reverse-transcribed using a high capacity cDNA reverse transcription kit (Applied Biosystems). The rat cDNAs were mixed with the forward and reverse primers of the target CYPs (CYP1A2, 2B2, 2C11, and 3A2), UGTs (UGT1A1, 1A2, 1A6, 1A7, and 1A8) or GAPDH and SYBR Green PCR master mix (Applied Biosystems). After an initial denaturation at 95 °C for 10 min, the amplification was performed by denaturation at 95 °C for 15 s and extension at 60 °C for 60 s, repeated for 50 cycles. The expression level of each mRNA was quantified by measuring the fluorescence intensity using the StepOnePlus real-time PCR system (Applied Biosystems) and was expressed as a ratio of GAPDH. The primer designs were referenced from various published articles [15–21], while the primer sequences and PCR product sizes were confirmed using primer-BLAST (http://www.ncbi.nlm.nih.gov/tools/primer-blast/).

2.4. MPAG formation in rat liver microsomes

Liver microsomes from control rats and NARs were prepared according to a commonly used procedure [22]. MPAG formation by liver microsomes was studied by the previously reported method [23] with a slight modification. Liver microsomes (1 mg) was incubated in buffer containing 75 mM Tris-hydrochloric acid (pH 7.45) and 10 mM magnesium chloride. The total volume was 50 μL, and the final concentration of MPA was 5–640 μg/mL. After pretreated with alamethicin (50 μg/mg) for 15 min on ice, reactions were initiated by the addition of uridine 5'-diphospho-glucuronic acid (3 mM final concentration) and were allowed to proceed at 37 °C for 30 min. Reactions were stopped by the addition of two volumes of the internal standard methanol solution. The amount of MPAG formed was measured, and kinetic parameters, the Michaelis–Menten constant (K_m; μg/mL) and the maximum velocity (V_{max}; ng/mg protein per 30 min), were determined using a non-linear least squares method (WinNonlin 6.4; Pharsight, Mountain View, CA).

2.5. Analytical methods

Concentrations of MPA and MPAG were analyzed using a reverse phase liquid chromatography-tandem mass spectrometry according to the previously reported method [24]. The limits of determination were 2 and 20 ng/mL for MPA and MPAG, respectively.

The PBMC samples were used to measure IMPDH activity according to the previously reported method [24] with a slight modification. Briefly, thawed PBMCs diluted with 200 μL of water were vortexed and centrifuged at 1000 *g* for 2 min. The reaction was initiated by adding 50 μL of supernatant to 52 μL of incubation mixture consisting of 1.6 mM phosphate buffer (pH 7.4), 3.9 mM potassium chloride, 4.8 mM inosine-5′-monophosphate disodium salt, and 0.6 mM NAD^+ as final concentrations. The mixture was incubated at 37 °C for 120 min. The reaction was stopped by the addition of 5 μL of 2.5 M perchloric acid followed by 10 μL of 3 M

potassium monohydrogen phosphate. The XMP and internal AMP in the supernatants were then determined by mass spectrometric measurements. The limits of determination were 50 and 100 ng/mL for XMP and AMP, respectively. The IMPDH activity was calculated based on the XMP produced, which was normalized to the intracellular AMP.

2.6. Pharmacokinetic and pharmacodynamic analysis

To characterize the differences in the time-course of MPA, pharmacokinetic and pharmacodynamic parameters in each rat were obtained by the non-compartmental analysis using the program WinNonlin 6.4. In addition, the simultaneous population pharmacokinetic and pharmacodynamic model analysis was performed to extract the changed pharmacokinetic and pharmacodynamic parameters in NARs and to simulate the effect of protein binding on the pharmacokinetics and pharmacodynamics of MPA (Supplemental Fig. 1). The MPA concentration was fitted to a 2-compartment model and the MPA was metabolized to MPAG by a first-order process. The MPA was assumed to completely convert to MPAG [25], and its concentration was described using a 1-compartment model with first-order elimination. The IMPDH activity was modeled using a sigmoid maximum inhibitory model based on the central free MPA concentration. The constructed model was parameterized based on the concentrations of free MPA and MPAG in order to fit both the control and NARs data simultaneously. The pharmacokinetic parameters estimated were the total body clearance of free MPA (CL_f), inter-compartment clearance of free MPA (Q_f), total body clearance of free MPAG (CL_{fMPAG}), central and peripheral volume of distribution of free MPA ($V_{c,f}$ and $V_{p,f}$, respectively), and volume of distribution of free MPAG (V_{fMPAG}). Each pharmacokinetic parameter of the total MPA or MPAG plasma concentrations were obtained by multiplying each parameter of the respective free concentrations by the free fraction of MPA or MPAG. In the mathematical calculation, the MPAG concentrations were converted to their equivalent MPA concentrations by dividing by 1.55. The pharmacodynamic parameters estimated were the half-maximal inhibitory concentration of free MPA ($IC_{50,f}$) as well as the Hill coefficient and baseline IMPDH activity ($IMPDH_0$).

Simultaneous pharmacokinetic and pharmacodynamic parameters were estimated using the nonlinear mixed effects modeling program NONMEM 7.2 with the ADVAN 7 subroutine by the first-order conditional estimation method with interaction [26]. The exponential and proportional error models were used for the interindividual and residual variability, respectively. In addition, each pharmacokinetic parameter "X" of the NAR group was modeled by multiplying the pharmacokinetic parameter "X" of the control by the factor (F_x); for example, CL_f of NARs was obtained by multiplying CL_f of the control by F_{CLf}. The statistical significance of each parameter such as the F_x, interindividual variability, and Hill coefficient was compared between two

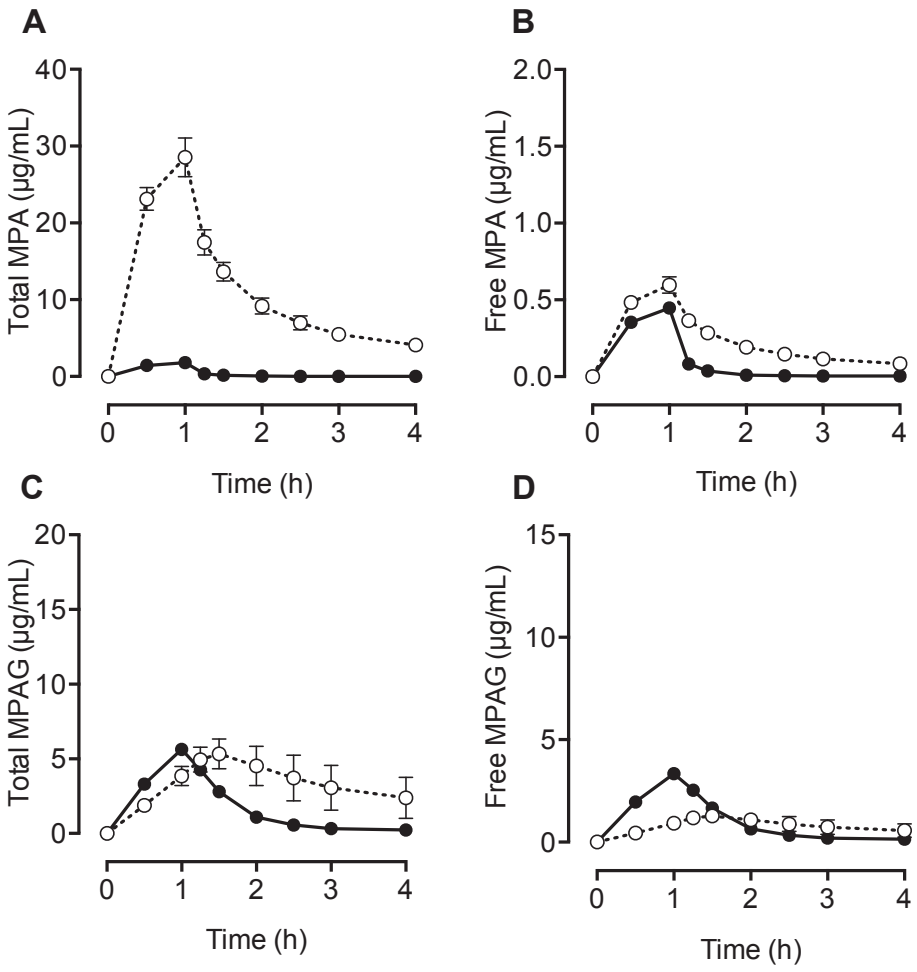

Fig. 1. Time-course of total MPA (A), free MPA (B), total MPAG (C), and free MPAG (D) concentrations. Each concentration was obtained after intravenous infusion of MPA at 5 mg/kg for 1 h in controls (open cycle) and NARs (closed cycle). Data are expressed as mean ± SEM of five rats.

models using the chi-squared test: for one model, the parameter of interest is freely estimated and for the other, the parameter should be set to an identical value such as zero or one. If the objective function value was not reduced by more than 7.88 in the former model compared to the latter model, the parameter to be estimated was fixed at zero or one ($P < 0.005$ with a freedom of 1 by chi-squared test).

2.7. Validation of model

The goodness-of-fit and visual predictive check plots were used for the internal validation of the final model. The goodness-of-fit plots consisted of observed *versus* population or individual predicted concentrations. The visual predictive check was performed as followed: the final pharmacokinetic-pharmacodynamic model was used to simulate original data sets at 1000 times. The 5th, 50th, and 95th percentiles of simulated data were compared with the observed data.

2.8. Simulation for effects of protein binding

The effects of protein binding on the pharmacokinetics and pharmacodynamics of MPA were evaluated using the simulation from the final pharmacokinetic-pharmacodynamic model and final parameters in control rats. One thousand data sets were simulated under the condition of the free fraction at 1, 2, 4, and 8%. In order to target the AUC_{0-4h} of MPA at 15 μg h/mL, the MPA doses were set at 0.675, 1.35, 2.7, and 5.4 mg/kg for the free MPA fraction at 1, 2, 4, and 8%, respectively. The AUC_{0-4h} of the total and free MPA, and the $AUEC_{0-4h}$ of IMPDH from the simulated data were calculated using the linear trapezoidal method.

2.9. Statistical analysis

All data were expressed as mean ± standard error of the mean (SEM). The statistical significance of the difference in mean values between the two groups was analyzed using an unpaired *t* test if the variance of the two groups were similar. Otherwise, the Mann–Whitney's U test was used for the analysis. A value of $P < 0.05$ was considered to be statistically significant.

Table 1
Pharmacokinetic and pharmacodynamic parameters of MPA after intravenous infusion (5 mg/kg) in controls and NARs by the non-compartmental analysis.

Parameters	Controls	NARs
Total MPA:		
C_{max} (μg/mL)	28.5 ± 2.5	1.80 ± 0.10***
AUC_{0-4h} (μg·h/mL)	46.0 ± 4.3	1.58 ± 0.07***
Free MPA:		
C_{max} (μg/mL)	0.597 ± 0.052	0.447 ± 0.024*
AUC_{0-4h} (μg·h/mL)	0.961 ± 0.089	0.393 ± 0.018***
Total MPAG:		
C_{max} (μg/mL)	5.54 ± 1.13	5.64 ± 0.37
AUC_{0-4h} (μg·h/mL)	13.2 ± 4.1	7.08 ± 0.68
Free MPAG:		
C_{max} (μg/mL)	1.33 ± 0.27	3.34 ± 0.22***
AUC_{0-4h} (μg·h/mL)	3.16 ± 0.97	4.20 ± 0.40
IMPDH activity:		
$IMPDH_0$ ($\mu mol \cdot sec^{-1} \cdot mol\ AMP^{-1}$)	97.9 ± 19.9	89.1 ± 25.4
$AUEC_{0-4h}$ ($\mu mol \cdot h \cdot sec^{-1} \cdot mol\ AMP^{-1}$)	153 ± 21	298 ± 68

C_{max}: maximum concentration of drug after administration, AUC: area under the concentration time curve, $IMPDH_0$: baseline IMPDH activity, AUEC: area under the effect time curve. *$P < 0.05$, ***$p < 0.001$, significantly different from controls by unpaired *t* test or Mann–Whitney's U test. Mean ± SEM, n = 5.

3. Results

3.1. Time-course of MPA and MPAG concentrations and IMPDH activity

The body weight of the NAR group was significantly lower than that of the controls at 236 ± 6 and 332 ± 16 g, respectively. The free fractions were significantly higher in the NARs than in the controls at 24.8 ± 2.6 and 2.09 ± 0.05% for MPA, and 59.3 ± 2.8 and 23.9 ± 4.0% for MPAG, respectively. There was no difference in the total protein concentrations measured by the Biuret method (5.18 ± 0.02 and 5.07 ± 0.05 g/dL in NAR and control groups, respectively).

The time-course of total or free MPA and MPAG concentrations after intravenous infusion of MPA (5 mg/kg) to the control and NAR groups are shown in Fig. 1, and the pharmacokinetic and pharmacodynamic parameters by the non-compartmental analysis were shown in Table 1. Although the maximum concentration (C_{max}) of total MPA in the NAR group was approximately 6% of that in the control rats, the C_{max} of free MPA in the NAR group was approximately 75% of that in the control rats (Fig. 1A, B and Table 1). The AUC_{0-4h} of total or free MPA was significantly lower in the NARs compared with that in the controls (Table 1). Although the C_{max} of total MPAG was similar in the control and NAR groups, the C_{max} of free MPAG in the NAR group was 2.5-fold higher compared with that in control rats (Fig. 1C, D and Table 1). The times corresponding to C_{max} for the total and free MPAG were shorter in NAR group than in the controls (Fig. 1C, D).

The time-course of IMPDH activity after an intravenous infusion of MPA (5 mg/kg) in the control and NAR groups are shown in Fig. 2. The IMPDH activity sharply decreased during the MPA intravenous administration for 1 h, and gradually recovered after the infusion. The $IMPDH_0$ and the $AUEC_{0-4h}$ of IMPDH activity were not significantly different between both groups of rats (Table 1).

3.2. Relationship between total or free MPA concentration and IMPDH activity

The relationships between the MPA concentration and IMPDH activity in the control and NAR groups are shown in Fig. 3. The IMPDH activity was inhibited by total and free MPA, concentration-dependently. Although the inhibition curve of the NAR group was

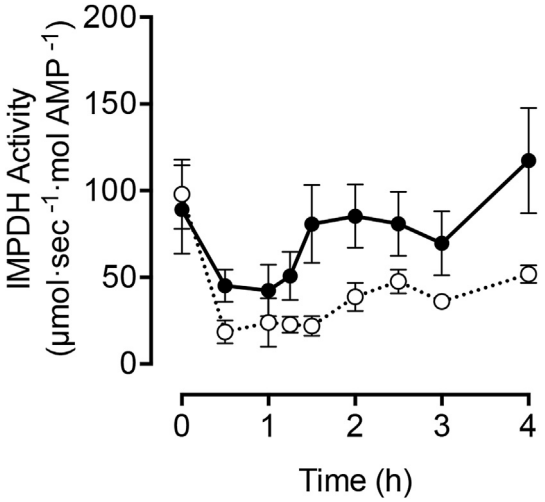

Fig. 2. Time-course of IMPDH activity. Each IMPDH activity was obtained after intravenous infusion of MPA at 5 mg/kg for 1 h in controls (open cycle) and NARs (closed cycle). Data are expressed as mean ± SEM of five rats.

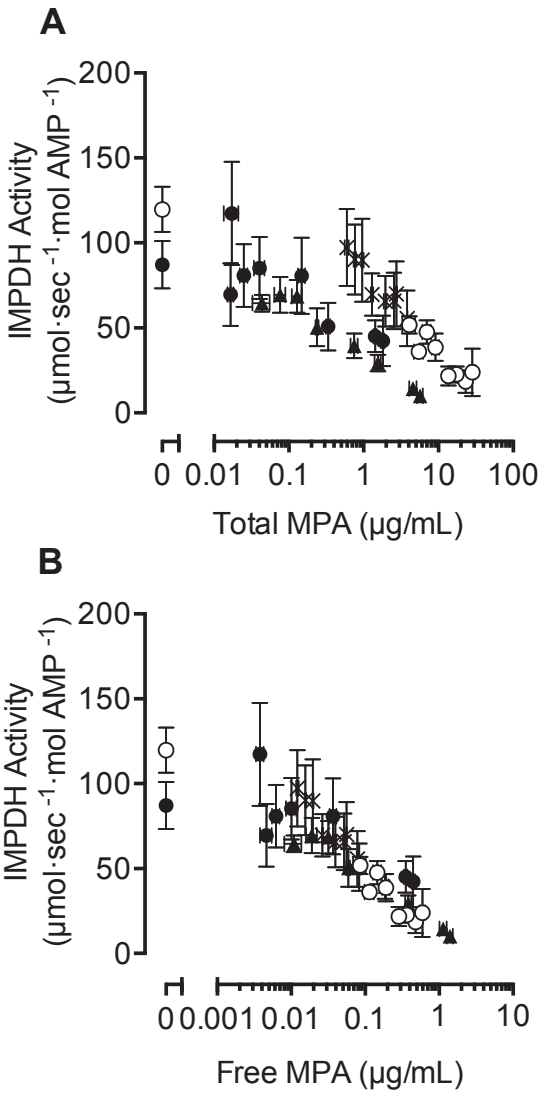

Fig. 3. Relationship between IMPDH activity and total (A) or free MPA concentrations (B). MPA was intravenously infusion for 1 h at 0.5 (cross) or 5 mg/kg (open cycle) in controls and 5 (closed cycle) or 15 mg/kg (closed triangle) in NARs. Data are expressed as mean ± SEM of five rats.

shifted to the left compared with that of the control group for the total MPA (Fig. 3A), the curves of both groups overlapped for the free MPA concentration (Fig. 3B).

3.3. mRNA expression of CYPs and UGTs and UGT activity in liver microsomes

We measured the mRNA expressions of four CYPs and five UGTs in the liver of both rats (Supplemental Fig. 2) and also determined the UGT activity in the liver microsomes. The mRNA expressions of CYP1A2 and 2B2 were significantly lower in the NAR group compared with the control (0.525-fold and 0.330-fold, respectively). Furthermore, the mRNA expression of UGT1A7 was significantly higher in the NAR group compared with the control (1.70-fold). The mRNA expressions of CYP2C11 and 3A2, and UGT1A1, 1A2, 1A6, and 1A8 were not significantly different between the control and NAR groups.

Kinetic parameters for MPA glucuronidation by liver microsomes were not significantly different between controls and NARs (K_m: 57.9 ± 0.9 *versus* 54.7 ± 9.1 μg/mL, V_{max}: 187 ± 44 *versus* 135 ± 37 ng min^{-1}·mg protein $^{-1}$, respectively).

3.4. Pharmacokinetic and pharmacodynamic modeling of MPA

The final estimates and its relative SEM for the pharmacokinetic and pharmacodynamic parameters by the non-linear mixed effects modeling are showed in Table 2. The CL_f in the control group was 3.61 L h^{-1}·kg^{-1}, and this value was significantly higher by 3.15-fold in the NAR group. In contrast, the Q_f, $V_{c,f}$, $V_{p,f}$, and V_{fMPAG} were significantly lower in the NAR group compared with the control group (0.304-, 0.782-, 0.421-, and 0.571-fold, respectively). The CL_{fMPAG} values were not significantly different between the control and NAR groups. The $IC_{50,f}$ and $IMPDH_0$ were estimated as 163 ± 13 ng/mL and 84.4 ± 13.7 μmol sec^{-1}·mol AMP^{-1}, respectively, and were not significantly different between both groups. A large interindividual variability was observed in the $IC_{50,f}$ at 96.4%. Since the Hill coefficient was not significantly different from one, the sigmoidal maximal inhibitory model was reduced to the maximal inhibitory model. The interindividual variability for the $V_{c,f}$ was not included in the final model by the result of the chi-squared test. Both the goodness-of-fit and visual predictive check plots for MPA and MPAG as well as IMPDH activity demonstrated that the final model reasonably described the observed pharmacokinetic and pharmacodynamic data for both groups (Figs. 4 and 5).

3.5. Simulation for effect of protein binding

The AUC of the total and free MPA as well as AUEC of the IMPDH activity were simulated using the final population pharmacokinetic

Table 2
Final pharmacokinetic and pharmacodynamic parameters of MPA in controls and NARs by the non-linear mixed effects modeling.

Parameters	Estimates	RSE (%)
Mean parameters:		
CL_f (L·h^{-1}·kg^{-1})	3.61	17.4
Q_f (L·h^{-1}·kg^{-1})	3.60	9.36
$V_{c,f}$ (L/kg)	3.04	10.8
$V_{p,f}$ (L/kg)	4.36	11.9
CL_{fMPAG} (L·h^{-1}·kg^{-1})	1.67	24.4
V_{fMPAG} (L/kg)	2.00	32.7
F_{CLf}	3.15	27.6
F_{Qf}	0.304	39.8
$F_{Vc,f}$	0.782	5.20
$F_{Vp,f}$	0.421	47.5
F_{VfMPAG}	0.571	47.3
$IC_{50,f}$ (ng/mL)	163	8.28
$IMPDH_0$ (μmol·sec^{-1}·mol AMP^{-1})	84.4	16.2
Interindividual variability (IIV: CV %):		
IIV for CL_f	16.0	36.5
IIV for Q_f	22.8	40.9
IIV for $V_{p,f}$	34.5	52.0
IIV for CL_{fMPAG}	41.7	47.0
IIV for V_{fMPAG}	23.5	40.3
IIV for $IC_{50,f}$	96.4	42.1
IIV for $IMPDH_0$	29.9	33.5
Residual variability (proportional error: CV %):		
MPA	12.3	20.7
MPAG	22.4	30.8
IMPDH activity	32.2	15.8

CL_f, total body clearance of free MPA; Q_f, inter-compartment clearance of free MPA; $V_{c,f}$, central volume of distribution of free MPA; $V_{p,f}$, peripheral volume of distribution of free MPA; CL_{fMPAG}, total body clearance of free MPAG; V_{fMPAG}, volume of distribution of free MPAG; $IC_{50,f}$, half-maximal inhibitory concentration of free MPA; $IMPDH_0$, baseline IMPDH activity; RSE, relative standard error; CV, coefficient of variation; F_X, fold increase of parameter "X" of NARs compared with that of controls (CL_f of NARs = $F_{CLf} \times CL_f$; Q_f of NARs = $F_{Qf} \times Q_f$; $V_{c,f}$ of NARs = $F_{Vc,f} \times V_{c,f}$; $V_{p,f}$ of NARs = $F_{Vp,f} \times V_{p,f}$; V_{fMPAG} of NARs = $F_{VfMPAG} \times V_{fMPAG}$; CL_{fMPAG} of NARs = CL_{fMPAG}).

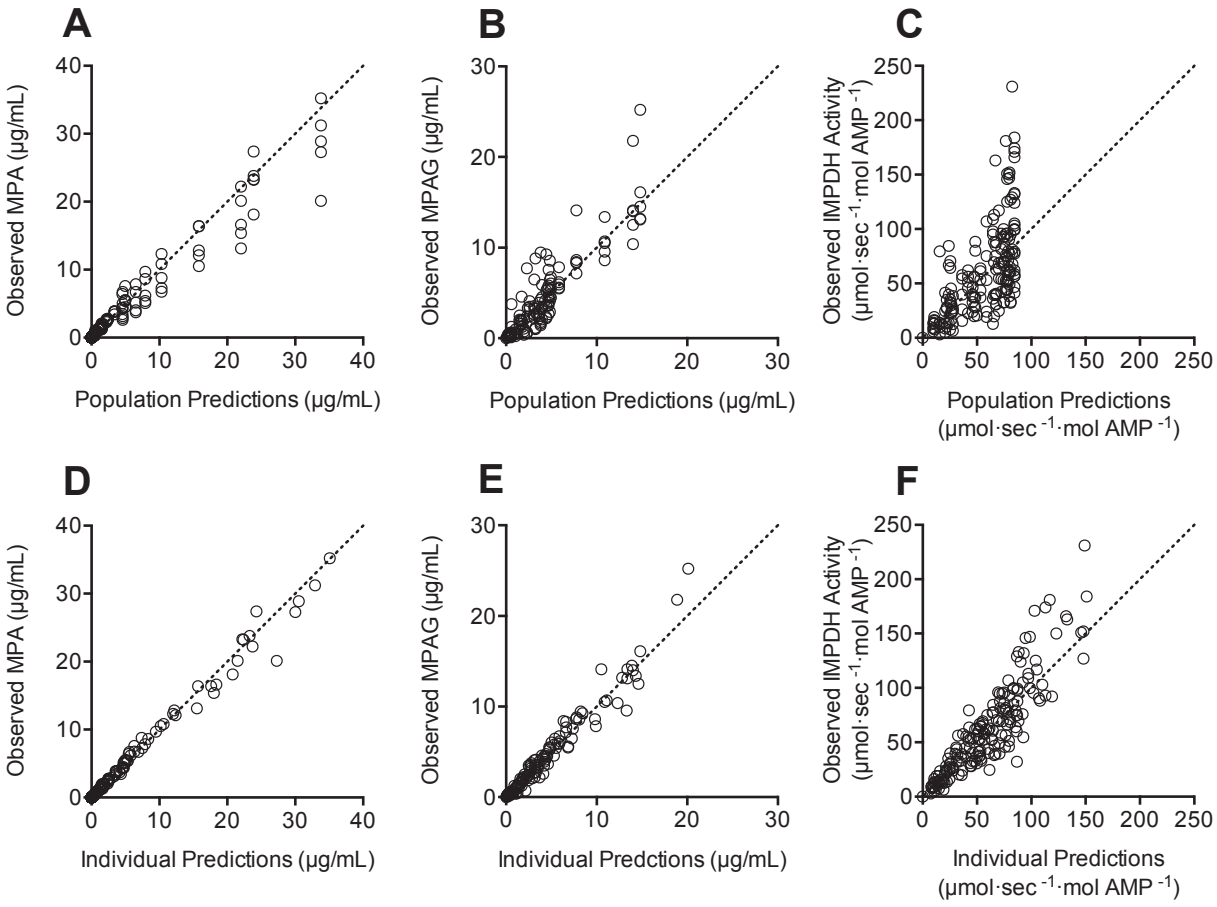

Fig. 4. Goodness-of-fit plots of observed *versus* population predictions (A–C) or individual predictions (D–F) using the final model. (A, D) MPA concentrations of controls and NARs. (B, E) MPAG concentrations of controls and NARs. (C, F) IMPDH activities of controls and NARs. Each dotted line shows the line of identity.

and pharmacodynamic parameters of the control, to examine the effect of the free fraction of MPA (Fig. 6). The AUC_{0-4h} of the free MPA increased linearly according to the increase in the free fraction of MPA (Fig. 6A). However, the $AUEC_{0-4h}$ of the IMPDH activity decreased non-linearly with a larger variability compared with that in the AUC_{0-4h} of the free MPA (Fig. 6B).

4. Discussion

The pharmacokinetics of MPA shows a large inter- and intra-individual variability and monitoring of its AUC after administration has been used in individualized therapy for organ transplantations [6,9]. The plasma protein binding of MPA is over 98% [7] and, therefore, its pharmacokinetics and pharmacodynamics could change in patients with hypoalbuminemia. In this study, the pharmacokinetics and pharmacodynamics of MPA were examined in NARs, and the modeling and simulation approach using these experimental data enables the quantitative assessment of the effects of protein binding on the associated IMPDH activity, as a biomarker of the pharmacodynamics of MPA.

The non-compartmental pharmacokinetic analysis following the intravenous administration of MPA showed that the AUC_{0-4h} of the total MPA in the NAR group was approximately 3% compared with that in the controls, and that of the free MPA was approximately 40% of the controls. Before the experiment, we speculated that the AUC_{0-4h} values of the free MPA in the NAR and control groups were similar, and that the pharmacokinetic differences in the NARs were mainly attributable to the higher free fraction of MPA. According to the simultaneous population pharmacokinetic and pharmacodynamic analysis, the CL_f of the NARs was 3.15-fold higher compared with that of the controls, indicating the intrinsic clearance was dramatically higher in NARs.

It has been reported that the recombinant rat UGT1A1, 1A6, and 1A7 showed MPA-glucuronization activity, and UGT1A7 showed the highest apparent activity followed by 1A6 and 1A1 [23]. In this study, we measured the mRNA expression levels of five UGTs and found that the mRNA expression of UGT1A7 was higher in the NAR group than in the control group. However, kinetic parameters for MPA glucuronidation by liver microsomes were not significantly different between controls and NARs. Therefore, precise mechanisms of increased intrinsic clearance in NARs were unknown and remain to be clarified in the future study.

The plasma free fraction of MPA was significantly higher in the NAR group by approximately 12-fold than in the controls (24.8 versus 2.1%), but not 100%. The plasma albumin level of the NAR group was barely detected at 0.0042% [27], but the concentrations of globulins were reported to be higher in the NARs than in the control rats [10]. Indeed, we confirmed that there was no difference in the total protein concentrations between two groups. Since approximately 30–40% of bumetanide was bound to rat α- and β-globulins in NARs [11], MPA also might be bound to globulins in the plasma of NARs. The $V_{c,f}$, $V_{p,f}$ and V_{fMPAG} significantly decreased in the NARs compared with the controls, indicating that the distribution as well as the hepatic intrinsic metabolism were changed in the NARs.

Concerning the pharmacodynamics, the inhibition curve for IMPDH activity against the free MPA concentrations was similar for

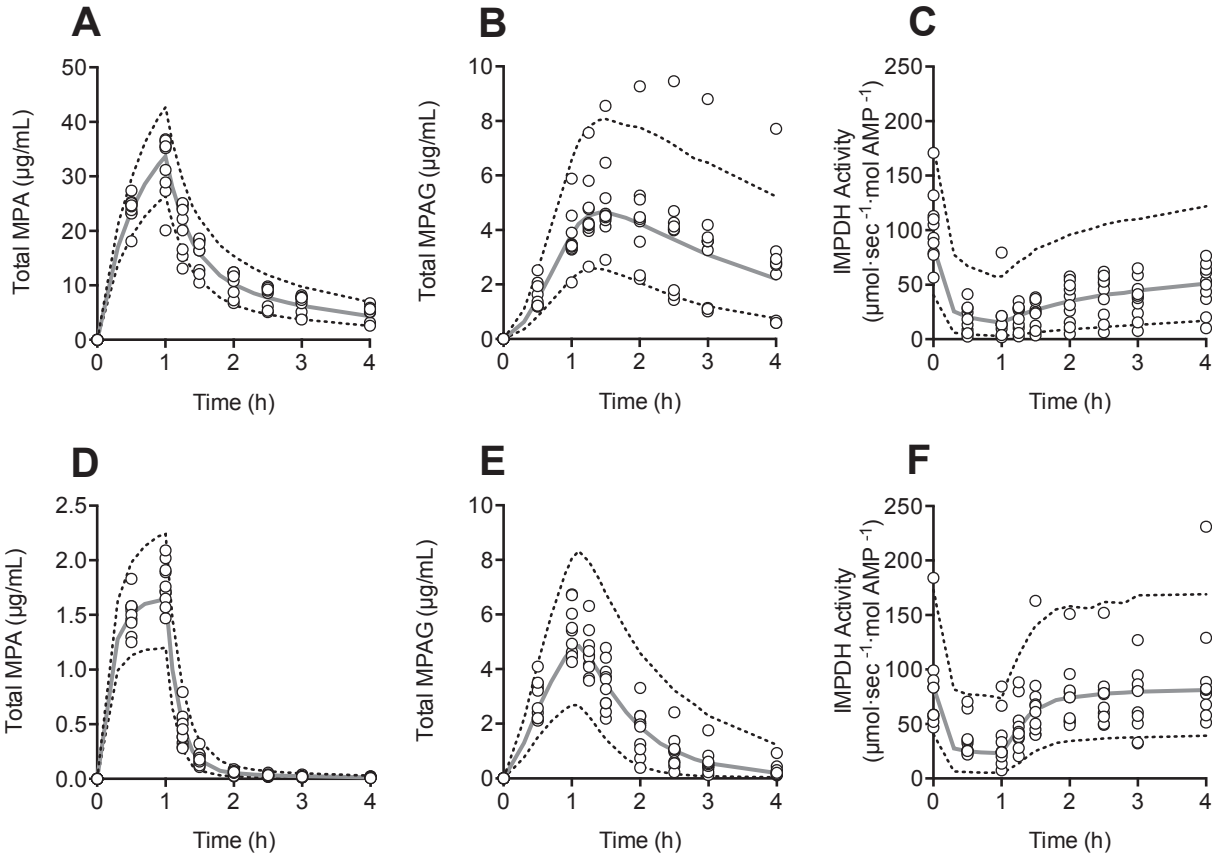

Fig. 5. Visual predictive check of MPA and MPAG concentrations and IMPDH activity in control rats (A–C) or NARs (D–F). (A, D) MPA concentrations. (B, E) MPAG concentrations. (C, F) IMPDH activities. Open circles shows observed data after intravenous infusion of MPA in 10 control rats or in 10 NARs. Although the MPA doses were 0.5 and 5 mg/kg for control and 5 and 15 mg/kg for NAR groups, each observed data was normalized to 5 mg/kg using the individual estimated pharmacokinetic and pharmacodynamic parameters. Dotted lines shows 5th or 95th percentile, and gray lines shows 50th percentile of 1000 simulated concentrations after intravenous infusion of 5 mg/kg of MPA using the final pharmacokinetic and pharmacodynamic parameters of the controls or NARs.

both groups, although NARs showed higher sensitivity compared with controls in the case of total MPA concentrations. According to the constructed population pharmacokinetic and pharmacodynamic model, the calculated IC_{50} value for free MPA was 163 ng/mL in both rats. These results indicated that the free MPA concentrations were better pharmacodynamic biomarker compared with the total MPA concentrations. The IC_{50} of MPA for the proliferation of rat PBMCs stimulated with T- or B-cell mitogens were reported as 241 nM (77 ng/mL) and 118 nM (38 ng/mL) for T- and B-cells, respectively [28], corresponding with our IC_{50} value.

In this study, we successfully constructed a simultaneous pharmacokinetic and pharmacodynamic model of MPA using the experimental data obtained from the control and NARs by the nonlinear mixed effects modeling approach. The predicted values of the final model corresponded reasonably well with the observed concentrations of MPA and MPAG, as well as the IMPDH activity in both groups of rats. The obtained parameters indicated that although the hepatic metabolism and distribution of free MPA were changed in the NARs, the pharmacodynamic sensitivity to free MPA was similar between NARs and control rats. The interindividual variability of the IC_{50} for free MPA was revealed to be as high as 96.4%, although the interindividual variability of the CL_f was as small as 16.0%. These results suggest that there might be a larger interindividual variability in the pharmacodynamics of MPA than in its pharmacokinetics in humans.

We quantitatively evaluated the effect of protein binding on the pharmacokinetics and pharmacodynamics of MPA using the final parameters of the control rats. Since the consensus target AUC_{0-12h} of MPA has been proposed as 30–60 μg h/mL in patients with renal transplants [6], we set the target AUC_{0-4h} of the total MPA to be 15 μg h/mL in the simulation study. In this situation, the AUC_{0-4h} of the free MPA will increase linearly from 0.15 to 1.2 μg h/mL based on the change in the free fraction of MPA from 1 to 8%. In contrast, the $AUEC_{0-4h}$ of the IMPDH activity will decrease non-linearly from 299 to 164 μmol h·sec^{-1}·mol AMP^{-1} with an increase in the free fraction of MPA from 1 to 8%. Patients with hepatic or renal transplants may suffer from hepatic or renal failure due to a relapse of the primary disease, rejection, or longitudinal adverse effects caused by calcineurin inhibitors. Renal or hepatic dysfunction decreases serum albumin. Thus, it is possible that increasing the dose of MPA based on the total AUC_{0-12h} might cause extra-immunosuppression, leading to an increase in adverse effects (for example, leukopenia and risk of infection), especially in patients with hypoalbuminemia.

In conclusion, the metabolism and disposition of free MPA were altered in the NARs compared with the control rats, in addition to the higher free fraction of MPA. We successfully constructed a simultaneous pharmacokinetic-pharmacodynamic model of MPA using a nonlinear mixed effects modeling approach, and the following simulation study quantitatively clarified an important issue concerning the free MPA concentration associated with the immunosuppressive effect. In patients with decreased protein binding of MPA, dosage adjustments that are based on the total AUC might cause unnecessary overexposure to MPA.

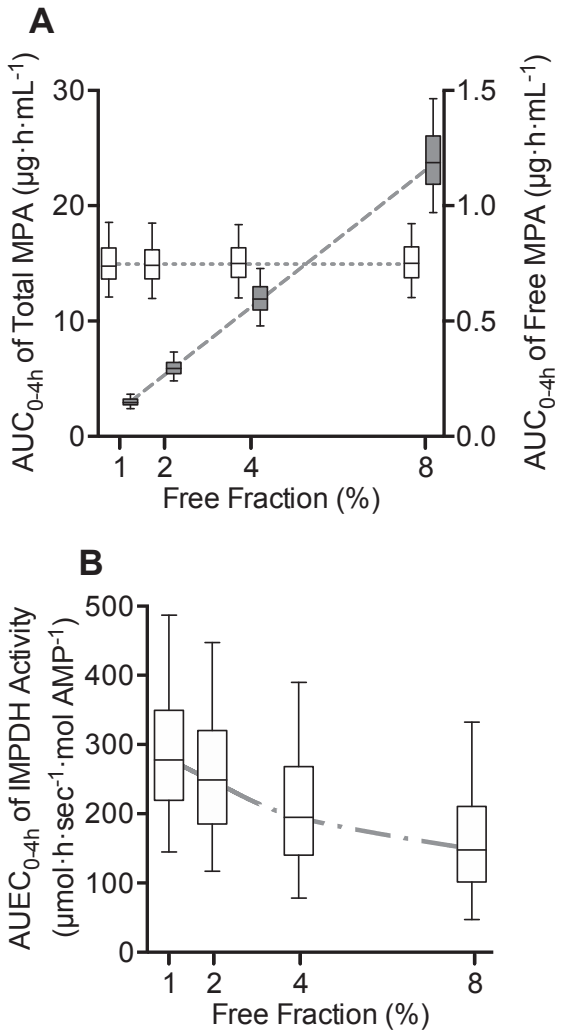

Fig. 6. Effect of free fraction on pharmacokinetics and pharmacodynamics of MPA. AUC_{0-4h} of total MPA was targeted at 15 μg h/mL, and MPA dose was set as 0.675, 1.35, 2.7, and 5.4 mg/kg for free fraction at 1, 2, 4, and 8%, respectively. (A) AUC_{0-4h} of total (white box) and free (grey box) MPA obtained from model simulations. (B) $AUEC_{0-4h}$ of IMPDH activity obtained from model simulations. Box plots represent the 5th percentile, lower quartile, median, upper quartile, and 95th percentile values obtained from 1000 simulated data sets.

Conflict of interest

None of the authors has any conflict of interest related to this study.

Acknowledgments

This study was supported in part by JSPS KAKENHI number 25460210.

Appendix A. Supplementary data

Supplementary data related to this article can be found at http://dx.doi.org/10.1016/j.dmpk.2015.10.004.

References

[1] Allison AC, Eugui EM. Mycophenolate mofetil and its mechanisms of action. Immunopharmacology 2000;47:85–118.
[2] Kaufman DB, Shapiro R, Lucey MR, Cherikh WS, Bustami RT, Dyke DB. Immunosuppression: practice and trends. Am J Transpl 2004;4:38–53.
[3] Minagawa K, Yamamori M, Katayama Y, Matsui T. Mycophenolate mofetil: fully utilizing its benefits for GvHD prophylaxis. Int J Hematol 2012;96:10–25.
[4] Premaud A, Le Meur Y, Debord J, Szelag JC, Rousseau A, Hoizey G, et al. Maximum A posteriori Bayesian estimation of mycophenolic acid pharmacokinetics in renal transplant recipients at different postgrafting periods. Ther Drug Monit 2005;27:354–61.
[5] Staatz CE, Tett SE. Clinical pharmacokinetics and pharmacodynamics of mycophenolate in solid organ transplant recipients. Clin Pharmacokinet 2007;46:13–58.
[6] van Gelder T, Hilbrands LB, Vanrenterghem Y, Weimar W, de Fijter JW, Squifflet JP, et al. A randomized double-blind, multicenter plasma concentration controlled study of the safety and efficacy of oral mycophenolate mofetil for the prevention of acute rejection after kidney transplantation. Transplantation 1999;68:261–6.
[7] Nowak I, Shaw LM. Mycophenolic-Acid binding to human serum-albumin – characterization and relation to pharmacodynamics. Clin Chem 1995;41:1011–7.
[8] Glander P, Hambach P, Braun K-P, Fritsche L, Giessing M, Mai I, et al. Pretransplant inosine monophosphate dehydrogenase activity is associated with clinical outcome after renal transplantation. Am J Transpl 2004;4:2045–51.
[9] Li H, Mager DE, Sandmaier BM, Storer BE, Boeckh MJ, Bemer MJ, et al. Pharmacokinetic and pharmacodynamic analysis of inosine monophosphate dehydrogenase activity in hematopoietic cell transplantation recipients treated with mycophenolate mofetil. Biol Blood Marrow Transpl 2014;20:1121–9.
[10] Nagase S, Shimamune K. Albumin-deficient rat mutant. Science 1979;205:590–1.
[11] Kim EJ, Lee MG. Pharmacokinetics and pharmacodynamics of intravenous bumetanide in mutant Nagase analbuminemic rats: importance of globulin binding for the pharmacodynamic effects. Biopharm Drug Dispos 2001;22:147–56.
[12] Kim EJ, Lee AK, Kim SH, Kim SG, Lee MG. Pharmacokinetics and pharmacodynamics of intravenous azosemide in mutant Nagase analbuminemic rats. Drug Metab Dispos 2003;31:194–201.
[13] Choi YH, Bae SK, Oh JM, Kim S-O, Lee MG. Pharmacokinetics of intravenous methotrexate in mutant Nagase analbuminemic rats. Biopharm Drug Dispos 2007;28:385–92.
[14] Miida H, Arakawa S, Shibaya Y, Honda K, Kiyosawa N, Watanabe K, et al. Toxicokinetic and toxicodynamic analysis of clofibrate based on free drug concentrations in Nagase analbuminemia rats (NAR). J Toxicol Sci 2008;33:349–61.
[15] Hebbar V, Shen GX, Hu R, Kim BR, Chen C, Korytko PJ, et al. Toxicogenomics of resveratrol in rat liver. Life Sci 2005;76:2299–314.
[16] Tian H, Ou J, Strom SC, Venkataramanan R. Activity and expression of various isoforms of uridine diphosphate glucuronosyltransferase are differentially regulated during hepatic regeneration in rats. Pharm Res 2005;22:2007–15.
[17] Omiecinski CJ, Hassett C, Costa P. Developmental expression and in situ localization of the phenobarbital-inducible rat hepatic mRNAs for cytochromes CYP2B1, CYP2B2, CYP2C6, and CYP3A1. Mol Pharmacol 1990;38:462–70.
[18] Iida J, Kudo T, Shimada K, Yatsuno Y, Yamagishi S, Hasegawa S, et al. Investigation of the safety of topical metronidazole from a pharmacokinetic perspective. Biol Pharm Bull 2013;36:89–95.
[19] Elbarbry FA, McNamara PJ, Alcorn J. Ontogeny of hepatic CYP1A2 and CYP2E1 expression in rat. J Biochem Mol Toxic 2007;21:41–50.
[20] Myers AL, Hassan HE, Lee IJ, Eddington ND. Repeated administration of oxycodone modifies the gene expression of several drug metabolising enzymes in the hepatic tissue of male sprague-dawley rats, including glutathione S-transferase A-5 (rGSTA5) and CYP3A2. J Pharm Pharmacol 2010;62:189–96.
[21] Ma J, Zheng L, Deng T, Li CL, He YS, Li HJ, et al. Stilbene glucoside inhibits the glucuronidation of emodin in rats through the down-regulation of UDP-glucuronosyltransferases 1A8: application to a drug-drug interaction study in radix polygoni multiflori. J Ethnopharmacol 2013;147:335–40.
[22] Kessler FK, Ritter JK. Induction of a rat liver benzo[a]pyrene-trans-7,8-dihydrodiol glucuronidating activity by oltipraz and beta-naphthoflavone. Carcinogenesis 1997;18:107–14.
[23] Miles KK, Stern ST, Smith PC, Kessler FK, Ali S, Ritter JK. An investigation of human and rat liver microsomal mycophenolic acid glucuronidation: evidence for a principal role of UGT1A enzymes and species differences in UGT1A specificity. Drug Metab Dispos 2005;33:1513–20.
[24] Kawanishi M, Yano I, Yoshimura K, Yamamoto T, Hashi S, Masuda S, et al. Sensitive and validated LC-MS/MS methods to evaluate mycophenolic acid pharmacokinetics and pharmacodynamics in hematopoietic stem cell transplant patients. Biomed Chromatogr 2015;29:1309–16.
[25] Bullingham R, Monroe S, Nicholls A, Hale M. Pharmacokinetics and bioavailability of mycophenolate mofetil in healthy subjects after single-dose oral and intravenous administration. J Clin Pharmacol 1996;36:315–24.
[26] Beal S, Boeckmann A, Sheiner L. NONMEM user's guides. NONMEM project group. San Francisco: University of California at San Francisco; 1992.
[27] Nagase S, Shimamune K, Shumiya S. Albumin-deficient rat mutant: an animal model for analbuminemia. Jikken Dobutsu 1980;29:33–8.
[28] Jain J, Almquist SJ, Heiser AD, Shlyakhter D, Leon E, Memmott C, et al. Characterization of pharmacological efficacy of VX-148, a new, potent immunosuppressive inosine 5′-monophosphate dehydrogenase inhibitor. J Pharmacol Exp Ther 2002;302:1272–7.